Global Medical Genetics 13 (2026) 100097

Contents lists available at ScienceDirect

Global Medical Genetics

journal homepage: www.keaipublishing.com/en/journals/global-medical-genetics/

Regulatory role and subtype analysis of m6A modifications in dermatomyositis

Xiang Long [a,1], Yidan Hu [b], Rui Tu [c,*,2], Youxian He [b,**,2]

[a] Department of Anesthesiology, The Affiliated Hospital, Southwest Medical University, Luzhou 646000, PR China
[b] Department of Rheumatology and Immunology, The Fourth Affiliated Hospital of Southwest Medical University, Meishan 620564, PR China
[c] Department of Anesthesiology, The Fourth Affiliated Hospital of Southwest Medical University, Meishan 620564, PR China

ARTICLE INFO

Article history:
Received 11 January 2026
Received in revised form 12 March 2026
Accepted 12 March 2026
Available online 14 March 2026

Keywords:
Dermatomyositis
N6-methyladenosine
m6A regulatory genes
machine learning

ABSTRACT

Background: Dermatomyositis (DM) is an uncommon autoimmune disease that presents challenges due to the lack of reliable biomarkers in clinical practice. Growing evidence suggests that N6-methyladenosine (m6A) is closely associated with the pathogenesis of autoimmune diseases.
Methods: Microarray gene expression matrix for GSE46239, GSE128314, and GSE142807 were downloaded from the GEO database. Random forest (RF), support vector machine (SVM), and nomogram models were developed, with their performance subsequently compared. The identification of m6A subtypes, based on differentially expressed m6A regulatory genes, was followed by the classification of gene subtypes according to the differently expressed genes between the m6A subtypes. Both classification systems were subjected to m6A scoring analysis and visualized via a Sankey diagram.
Results: We retrieved 99 dermatomyositis samples and 14 healthy samples. Using an RF model, we identified five core genes—IGFBP3, ZCCHC4, HNRNPC, WTAP, and RBM15—and constructed a predictive nomogram model. Two m6A clusters were developed. Cluster A exhibited a significant increase of CD56-bright natural killer cells, immature B cells, plasmacytoid dendritic cells, regulatory T cells, and type 1 T helper cells distinct from cluster B ($p < 0.05$). Based on 32 significantly distinctly expressed genes between m6A subtypes ($p < 0.05$), we further reproduced two m6A gene subtypes. The Sankey diagram showed significant concordance among m6A scores, m6A subtypes, and m6A gene subtypes.
Conclusion: m6A regulatory genes significantly influence the pathogenesis of dermatomyositis. In this work, we built a predictive nomogram model, comprehensively evaluated two classification methods, and provided new insights for patient classification.

Introduction

Dermatomyositis (DM) is an uncommon idiopathic connective tissue disease with multiple autoantibodies [1]. The condition is primarily characterized by marked skin lesions and myopathy, but also extends to other clinical features [2], including Arthritic pain, calcium deposits, pulmonary interstitial changes, malignant tumors, and gastrointestinal discomfort [3]. The etiology and pathogenesis of dermatomyositis are broadly involved and may consist primarily of environmental, genetic susceptibility, and immunologic factors [4]. Both immunologic disorders and genetic factors associated with dermatomyositis have been explored in previous studies [5]. Immune cells (including CD4 + T cells, B cells, natural killer (NK) cells, and macrophages, among others) have been reported to be abnormal both qualitatively and quantitatively in the tissues and circulation of DM patients [6].In addition, patients with dermatomyositis carry autoantibodies targeting the nucleus or cytoplasm of cells [7],

Abbreviations: RF, random forest; SVM, support vector machine; M6A, N6-methyladenosine; DM, dermatomyositis; TIF1 γ, anti-transcription intermediary factor 1 γ; NXP2, anti-nuclear matrix protein 2; SAE, anti-small ubiquitin-like modifier activating enzyme; MDA5, anti-melanoma differentiation antigen 5; DEGs, differentially expressed genes; ROC, receiver operating characteristic; DCA, decision curve analysis; CDF, cumulative distribution function; SsGSEA, Single-Sample Gene Set Enrichment Analysis; GO, Gene Ontology; KEGG, Kyoto Encyclopedia of Genes and Genomes

Peer review under responsibility of Editorial Board of Global Medical Genetics.

* Correspondence to: Department of Anesthesiology, The Fourth Affiliated Hospital of Southwest Medical University. No.168, Huantianfuxinqu Expressway, Meishan Tianfu New District, Meishan, Sichuan, PR China.
** Correspondence to: Department of Rheumatology and Immunology, The Fourth Affiliated Hospital of Southwest Medical University, No.168, Huantianfuxinqu Expressway, Meishan Tianfu New District, Meishan, Sichuan, PR China.
E-mail addresses: 710496030@qq.com (R. Tu), 583460032@qq.com (Y. He).
[1] First author
[2] Youxian He and Rui Tu jointly supervised this project, should be considered co-corresponding authors.

https://doi.org/10.1016/j.gmg.2026.100097

including anti-transcription intermediary factor 1 γ (TIF1 γ), anti-nuclear matrix protein 2 (NXP2), anti-small ubiquitin-like modifier activating enzyme (SAE), and anti-melanoma differentiation antigen 5 (MDA5) antibodies [8]. These abnormally activated immune cells and autoantibodies may ultimately cause organ system damage; however, the exact mechanism is not yet known.

Epigenetics encompasses heritable regulation of gene expression through chemical modifications to DNA and histones, and noncoding RNA activity, without altering the DNA sequence itself [9]. As one of the most prevalent modifications in eukaryotic RNAs [10,11], N6-methyladenosine (m6A) regulates diverse cellular processes by modulating the transcription, maturation, localization, function, and metabolism of RNA species [12]. This modification closely governs immune cell development, activation, and differentiation [13]. As a reversible biological process, m6A dynamically modulated through m6A "writers," "readers," and "erasers" [14]. Notably, the m6A writer, methyltransferase-like 3(METTL3), is essential for the generation of hematopoietic and immune cell lineages [15]. Furthermore, delayed mRNA decay of the arterial endothelial gene Notch Receptor 1 (Notch1a), mediated by m6A, its reader YTHDF2, exacerbates the impaired emergence of hematopoietic stem and progenitor cells [16,17].

m6A modifications are implicated in the pathogenesis of autoimmune diseases, including rheumatoid arthritis (RA) [18,19], systemic lupus erythematosus (SLE) [20], type 1 diabetes mellitus [21], and multiple sclerosis [22]. However, the role of m6A modification in the DM pathogenesis remains incompletely clear. In this research, we thoroughly explored the biological functions and immune properties of m6A modification in DM samples.

We identified five core m6A regulatory genes (IGFBP3, ZCCHC4, HNRNPC, WTAP, and RBM15) and developed a nomogram model for predicting DM incidence. Our work comprehensively analyses the role of m6A in DM for the first time, revealing consistent results between two distinct typing approaches. These findings may provide a new horizons for the therapy and diagnosis of DM.

Materials and methods

Data download and processing

Microarray gene expression data for GSE46239, GSE128314, and GSE142807 were downloaded from the GEO database (https://www.ncbi.nlm.nih.gov/geo/), which contains 99 DM samples in the DM group and 14 healthy samples in the control group. Information about the above GEO dataset is presented in Supplementary Table 1. We preprocessed all datasets via the R language “impute” and “limma”. Gene symbols were annotated with gene probes. To ensure data comparability and stabilize variance, Gene expression levels were log2-transformed before analysis, and all figures depicting expression values display these log2-transformed data. And we performed quantile normalization using the normalize between arrays function from the “limma” package. Subsequently, we merged the three datasets and applied the “ComBat” algorithm from the “sva” package to remove batch effects. After batch correction, samples were annotated as “Control” or “DM” according to their original group information. The complete flowchart of bioinformatic analysis and research design is shown in Fig. 1.

Screening for differentially expressed genes

Through a systematic review of the paper and the m6A2Target database [23] (http://m6A2target.canceromics.org), we identified 27 m6A RNA methylation regulatory genes [24]. Only 24 of these genes were detected in the merged dataset. Differentially expressed genes (DEGs) between DM samples and healthy samples were collected by the R language “dplyr”, and DEGs were visualized via drawing a volcano plot and a heatmap. Threshold values (log2 fold change (FC)) > 0.585, and we defined an adjusted P value of less than 0.05 as statistically significant.

Correlation analysis of DM-associated m6A regulatory genes

m6A regulatory genes were mapped to DEGs. The overlapping genes—differentially expressed m6A regulatory genes—were defined as DM-associated regulatory genes. We visualized the expression levels of these group-specific m6A regulatory genes through heatmaps and box plots. To investigate the functional interactions among these expressed m6A regulatory genes, we performed correlation analysis using their expression profiles in all DM samples with the R package “corrplot”, and subsequently identified co-expressed genes for these regulatory genes.

Construction of Random Forests (RF), Support Vector Machines (SVM), and nomogram models

To address the sample imbalance in the training set, the “ROSE” package was employed for correction. We adopted random forest (RF) and support vector machine (SVM) models to identify core genes among differentially expressed m6A-regulated genes. These models were trained with the balanced training set and validated with 5-fold cross-validation repeated three times. The evaluation of model accuracy was performed by employing three methods: residual boxplots, reverse cumulative distribution plots of residuals, and receiver operating characteristic (ROC) curves. The RF model was implemented via the R package “randomForest”, and assessed five alternative mtry values with tuneLength = 5, automatically. The importance of the core genes was assessed based on the optimal *ntree* configuration. Generating a nomogram model for predicting the occurrence of DM using the R package “rms”. Calibration charts are used to make comparisons between predicted and observed outcomes. To evaluate the model’s potential for improving patient benefit, we performed a decision curve analysis (DCA) and generated a clinical impact curve.

Immune correlation and consensus clustering analysis

Utilizing the various expression levels of m6A regulatory genes, we applied the "ConsensusClusterPlus" R package to stratify DM patients via unsupervised consensus clustering. Optimal subtype classification was guided by consensus cumulative distribution function (CDF) curves. Principal component analysis (PCA) was subsequently conducted to verify differences in expression among the identified subtypes.

Furthermore, we calculated the infiltration landscape of immune cells for different subtypes using Single-Sample Gene Set Enrichment Analysis (ssGSEA) and further conducted immune correlation analyses to generate heatmaps and boxplots for visualization. Based on the resulting immune profiles, we analyzed associations between immune cell features and the expression levels of the m6A regulatory genes Heterogeneous Nuclear Ribonucleoprotein A2/B1 (HNRNPA2B1) and RNA Binding Motif Protein 15B (RBM15B), with differential expression patterns illustrated in boxplots.

Enrichment analysis

To reveal the m6A modification patterns and pathways, differentially expressed genes between subtypes were discovered and subjected to Gene Ontology (GO) enrichment analysis and Kyoto Encyclopedia of Genes and Genomes (KEGG) enrichment analysis, using the R package “clusterProfiler”.

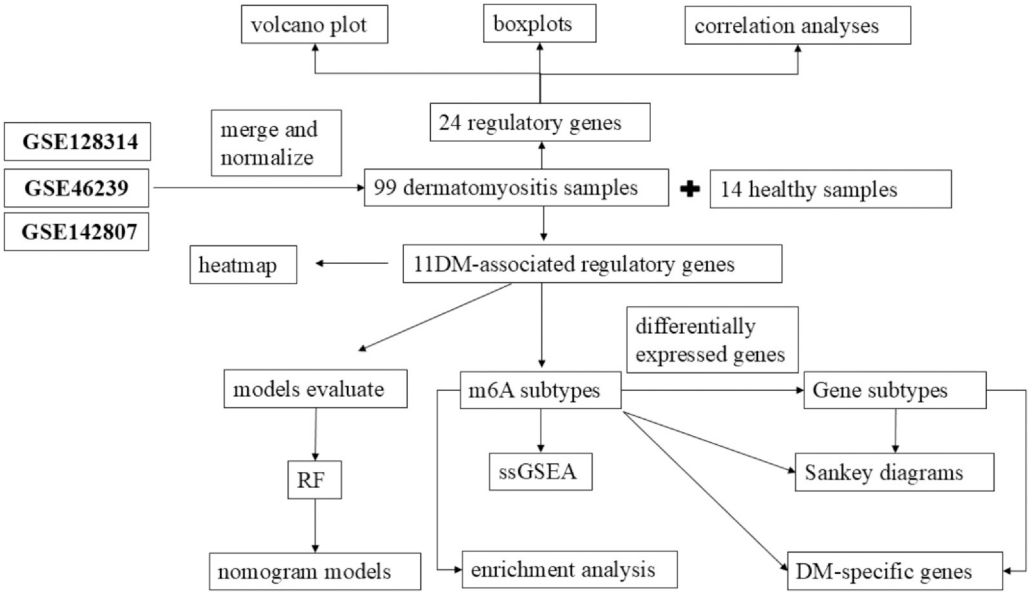

Fig. 1. Flowchart of bioinformatic analysis and research design.

Gene subtypes and m6A score calculation

We then performed unsupervised consensus clustering to categorize the DM samples into distinct gene subtypes based on the previously identified differentially expressed genes and plotted heatmaps accordingly. DM-associated m6A regulatory genes and immune properties were comparatively evaluated between gene subtypes, with differences visualized via boxplots. The m6A pattern was characterized by principal component analysis (PCA). Subsequently, we obtained the m6A score. Differential m6A scores between subtypes and gene subtypes were compared. Sankey diagrams visualizing the distribution patterns and consistency of m6A scores across subtypes and gene subtypes were generated via the R packages “ggalluvial”, “ggplot2”, and “dplyr”.

Analysis of DM-specific genes across subtypes and gene subtypes

Additionally, the differential expression of the GBP1, IFIH1, IFIT3, and BST2 genes between subtypes and gene subtypes was analyzed, with comparative boxplots generated to illustrate the findings.

Statistical analysis

Statistical analyses were performed using R software (version 4.x). For comparisons between two groups, the Wilcoxon rank-sum test was applied. For comparisons involving more than two groups, the Kruskal-Wallis test was first used to assess overall differences, followed by pairwise Wilcoxon rank-sum tests with Benjamini-Hochberg adjustment for multiple testing to control the false discovery rate. All statistical tests were two-sided, and a p-value < 0.05 was considered statistically significant. The significance levels were indicated as follows: *p < 0.05, **p < 0.01, ***p < 0.001.

Results

DM-associated m6A regulatory genes

In this research, the dataset was merged and normalized for PCA, as shown in Fig. 2A, B. We compared the DEGs between the DM and healthy samples, as presented in the volcano plot (Fig. 2E). Among the 27 m6A RNA methylation regulatory genes, 24 were exhibited in skin cells, and 11were expressed differently between the control group and the DM group (Fig. 2C). Moreover, we observed that genes Methyltransferase 3, N6-Adenosine-Methyltransferase Complex Catalytic Subunit (METTL3), Methyltransferase 14, N6-Adenosine-Methyltransferase Non-Catalytic Subunit (METTL14), WT1 Associated Protein (WTAP), RNA Binding Motif Protein 15 (RBM15), YTH N6-Methyladenosine RNA Binding Protein C2 (YTHDC2), Heterogeneous Nuclear Ribonucleoprotein C (HNRNPC), Fragile X Messenger Ribonucleoprotein 1 (FMR1), and Heterogeneous Nuclear Ribonucleoprotein A2/B1 (HNRNPA2B1) were significantly increased in the DM samples, whereas RBM15B, zinc finger CCHC-type containing 4 (ZCCHC4), and insulin like growth factor binding protein 3 (IGFBP3) were significantly increased in the healthy samples ($P < 0.05$) (Fig. 2D). Using the R package “corrplot”, the correlation analysis results of expression profiles across all dermatomyositis samples are shown in Fig. 2F.

The RF, SVM, and nomogram models

We constructed RF and SVM models and identified 5 core genes to predict the incidence of DM. The R package “DALEX” was used to measure the RF and SVM models. The residual box plots (Fig. 3A), the inverse cumulative distribution of the residuals (Fig. 3B), and the ROC curves (Fig. 3C) indicate that the RF model results in lower residuals than the SVM model does. Consequently, the RF model was adopted. The importance of m6A genes was prioritized by RF model, with the top five considered core genes (Fig. 3D, E).

Using these genes, we developed a predictive nomogram model for forecasting the prevalence of DM (Fig. 4A). As illustrated in Fig. 4 B, the calibration curve revealed concordance between the observed data and the ideal prediction line. The decision curve analysis reveals a deviation in the red line, which represents m6A regulatory genes, from both the gray and black lines. (Fig. 4D) The clinical impact curve shows that the curve for high-risk patients is positioned higher than that for DM patients (Fig. 4C).

Subtype analysis after consensus clustering

The R package “ConsensusClusterPlus” was utilized to analyze m6A subtypes based on 11 differentially expressed m6A-regulated genes. According to the CDF curves and PCA results (Fig. 5 B, C), K= 2

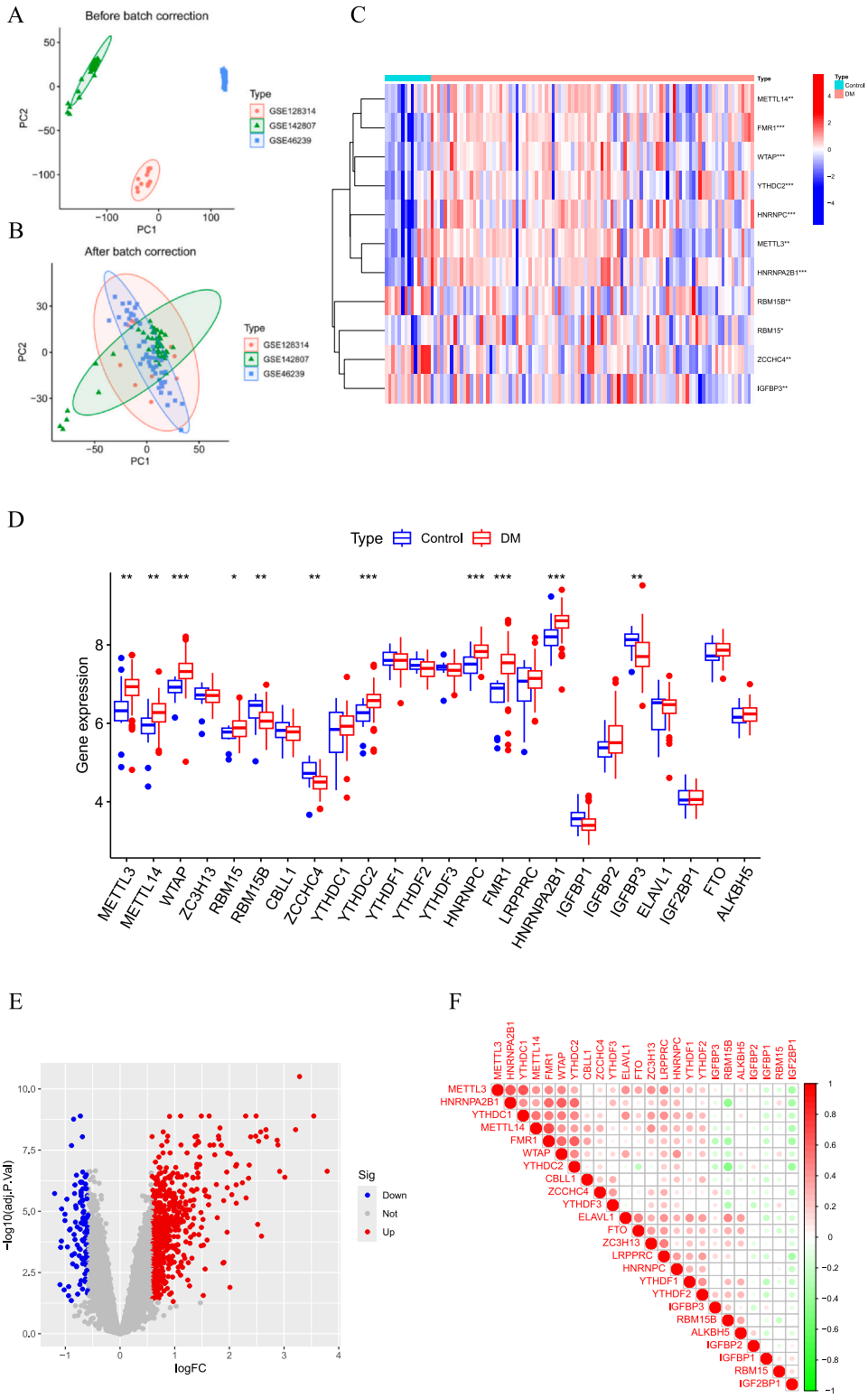

Fig. 2. m6A regulatory genes in dermatomyositis groups and healthy groups. (A) PCA of the three datasets before batch effect correction using "ComBat". (B) PCA of the integrated dataset after batch effect removal with "ComBat". The dataset contains 99 DM samples and 14 healthy samples. (C) Heatmap of M6a DEGs. (D)A boxplot illustrates the expression profile across the 24 m6A regulatory genes ("DM vs. CON"). (E) A volcano plot identifying differentially expressed genes in DM samples compared to healthy controls. Threshold values (log2 fold change (FC)) > 0.585, and we defined an adjusted P value of less than 0.05 as statistically significant. (F)Correlation analysis of the m6A regulatory genes in DM samples. *p < 0.05, **p < 0.01, and ***p < 0.001.

exhibited the optimal clustering performance (Fig. 5 A). Consequently, the DM samples were categorized into two subtypes, A and B. Heatmap and boxplot revealed that METTL3, METTL14, WTAP, YTHDC2, HNRNPC, FMR1, and HNRNPA2B1 exhibited significantly higher expression levels in subtype A than B, while RBM15B had the opposite pattern (Fig. 5D, E).

We compared the diversity in immune cell abundance between subtypes A and B. The divergences among CD56 bright natural killer

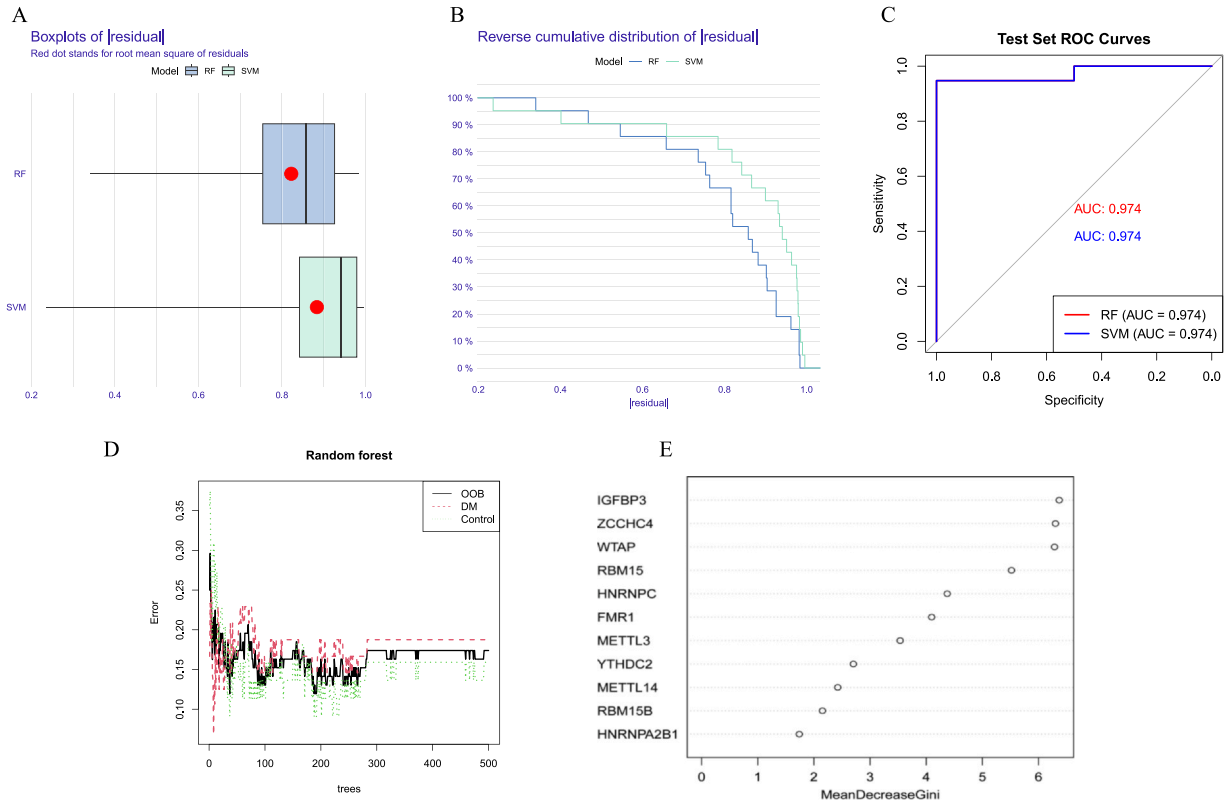

Fig. 3. Machine learning model. (A) Residual boxplots for two machine learning models. (B) Residual distributions for two machine learning models. (C) A predictive value of 0.974 was achieved by both the RF and SVM models, as shown in the ROC curves. (D) The red curve represents the error levels of the DM cluster, the green curve represents the control cluster, and the black curve represents all samples. (E) The Importance scores of 11 m6A regulatory genes.

cells, CD56 dim natural killer cells, immature B cells, plasmacytoid dendritic cells, regulatory T and type 1 T helper cells were statistically significant between subtypes A and B (Fig. 6A). Excluding CD56 dim natural killer cells, the remaining observed immune cells presented significantly higher infiltration levels in subtype A than in subtype B.

In addition, we investigated the correlation of 11 DM-associated m6A regulatory genes with immune cell infiltration. These conclusions indicated that HNRNPA2B1, WTAP, and RBM15 were positively correlated with most observed immune cells, whereas RBM15B was negatively correlated (Fig. 6B). Similar results were found in the immune cell infiltration analysis for HNRNPA2B1 and RBM15B. The overwhelming majority of immune cells in samples with high HNRNPA2B1 expression were noted to have a high degree of infiltration (Fig. 6D), whereas samples with high RBM15B expression showed low infiltration levels of most immune cells (Fig. 6C).

Differential analysis between subtypes and gene subtypes

We screened for genes that were differentially expressed between the two subtypes. These differentially expressed genes were subjected to Gene Ontology (GO) and Kyoto Encyclopedia of Genes and Genomes (KEGG) enrichment analyses. It was discovered that 32 genes were significantly differentially expressed between the two subtypes, and they were mainly enriched in the following processes:

In the biological processes (BP), differentially expressed genes were mainly associated with the viral response and the defense response to viruses. In cellular components (CC), differentially expressed genes were mainly located in keratin filaments, intermediate filaments, intermediate filament cytoskeletons, etc. In molecular function (MF), they are primarily involved in cytokine activity and cytokine receptor binding, etc (Fig. 7A). KEGG analysis indicated that the differentially expressed genes were significantly enriched for influenza A (Fig. 7B).

Based on the differentially expressed genes identified between the two m6A subtypes, DM patients were stratified into gene subtype A and gene subtype B (Fig. 8A). Heatmap visualizations revealed elevated expression levels of these genes in gene subtype A contrast to those in gene subtype B (Fig. 8B). We constructed boxplots based on m6A regulatory genes associated with dermatomyositis (Fig. 9A). The results revealed conspicuous diversity in the expression levels of METTL14, WTAP, RBM15B, YTHDC2, FMR1, and HNRNPA2B1 between the two gene subtypes, except for RBM15 B. All of these genes were markedly upregulated in subtype A. Furthermore, ssGSEA analysis showed significantly greater enrichment of most immune cells in gene subtype A compared to gene subtype B (Fig. 9B).

We further compared the m6A scores between the two m6A subtypes and the two gene subtypes. There were significant differences in the m6A scores between the two subtype classifications (Fig. 10 A, B). The Sankey diagram shows the consistency of m6A subtypes, gene subtypes, and m6A scores (Fig. 10D).

Relationships between specific genes and different subtypes

Previous studies identified GBP1, IFIH1, IFIT3, and BST2 [25]as genes closely associated with nasopharyngeal carcinoma in dermatomyositis patients. We further analyzed the expression of these genes across both m6A subtypes and gene subtypes. The conclusion illustrated a marked increase in the expression of all four genes in subgroup A relative to subgroup B, which was consistently observed under both classifications (Fig. 11A, B).

Discussion

Dermatomyositis is an idiopathic inflammatory disease that is mainly notorious for varying degrees of skin manifestations [26,27]. It impacts 1.2–17 individuals per 100,000 people [28], peaking in

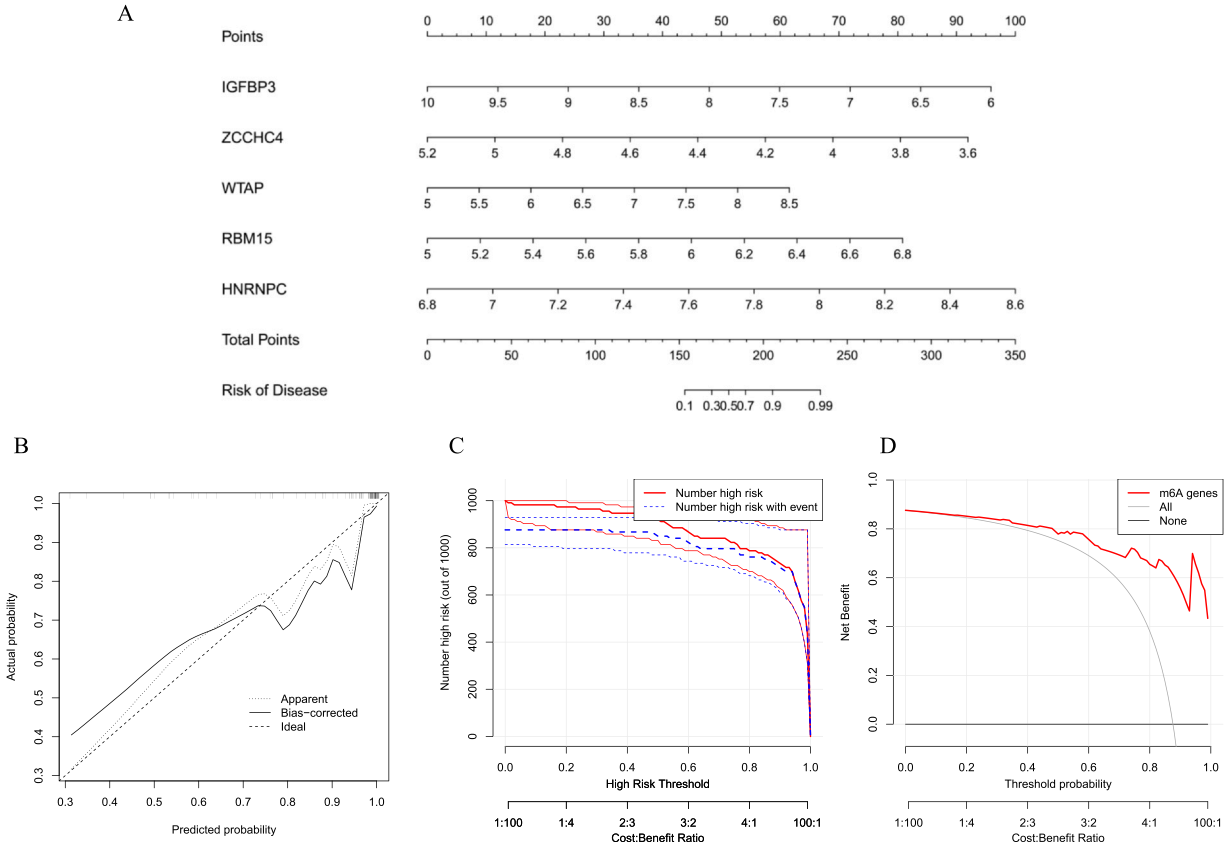

Fig. 4. The nomogram model. (A) The predictive incidence of five core m6A regulatory genes according to the total points of the nomogram model. (B) The solid line representing actual observation data and the dashed line representing ideal prediction data are close to each other. (C) Solid lines represent high-risk DM patients, whereas dashed lines represent DM patients. An assessment of the model's potential clinical utility is provided by the clinical impact curve. (D) The decision curve illustrates the model's feasibility.

children aged 5–15 years [29] and in adults at aged 45–65 years [30,31].However, owing to the complex and heterogeneous pathogenesis of dermatomyositis, there is a lack of universally effective treatments and reliable biomarkers. Recent research has focused on epigenetics, which regulates gene expression without affecting the DNA sequence [32]. m6A is the most universal epigenetic modification. This invertible process mainly relies on three m6A regulatory proteins, including "write proteins" (methyltransferases), "erase proteins" (demethylases), and "read proteins" (m6A binding proteins) [14]. Accumulating evidence indicates that m6A modifications play vital roles in disease inflammatory responses and the pathogenesis of certain autoimmune disorders [33,34]. However, there is no study that has reported m6A in dermatomyositis. In this study, we innovatively investigated the role of m6A regulatory genes in DM. We constructed a nomogram model to predict the incidence of dermatomyositis and categorized patients with dermatomyositis according to m6A regulatory genes, which will contribute to DM treatment and evaluation.

We screened 11 m6A regulatory genes among a total of 27 genes that were variously expressed between DM patients and healthy controls, including METTL14, FMR1, WTAP, YTHDC2, HNRNPC, METTL3, HNRNPA2B1, RBM15B, RBM15, ZCCHC4, and IGFBP3. Based on their differential expression, we hypothesized that these 11 genes may be involved in the pathogenesis of dermatomyositis. ZCCHC4, RBM15B, and IGFBP3 expression is downregulated in DM samples. Some studies suggest that these genes may be involved in the immune and inflammatory processes. METTL14 exhibits abnormal expression in multiple autoimmune diseases, including rheumatoid arthritis (RA), systemic lupus erythematosus (SLE), ulcerative colitis (UC), and Crohn's disease (CD) [35–38]. In peripheral blood and synovial tissue of RA patients, elevated METTL14 expression correlates with levels of CRP, RF, and other markers, promoting pro-inflammatory polarization of macrophages. Our findings show a similar trend to rheumatoid arthritis. In PBMCs from SLE patients, this is manifested as downregulation[37]. Research has found that WTAP is upregulated in airway epithelial cells from asthma patients, enhancing Wnt/β-catenin signaling and promoting the proliferation of airway smooth muscle cells [39]. RBM15 and RBM15B are homologues that interact with METTL3 in a WTAP-dependent manner, and their deletion impairs site-specific gene silencing [40]. METTL3 silencing inhibits the NF-κB pathway and further suppresses fibroblast proliferation, migration, invasion, and IL-6 expression [41]. This process may play a similar role in DM. It has been reported that IGFBP3 is connected to various autoimmune diseases. In rheumatoid arthritis synovium, IGFBP3 is produced by macrophages, whose expression in synovial fluid correlates with systemic levels of C-reactive protein (CRP), possibly suggesting inflammatory involvement [42]. In this study, its expression was downregulated. Significant differences were observed in the expression patterns and functional effects of these genes among different diseases.HNRNPA2B1 overexpression is associated with poor breast cancer prognosis and immune cell subsets [43].In non-small cell lung cancer, HNRNPC knockdown enhances immune cell infiltration, particularly that of CD8 + and CD4 + T cells [44].

Through machine learning, we identified the core genes among these 11 genes and constructed a nomogram model. In this study, we employed the random forest model because of its smaller residuals. The nomogram model built with core genes provides a convenient method for predicting dermatomyositis risk at the gene expression level. To our knowledge, this is the first predictive model constructed, although experimental validation with a large number of samples remains necessary.

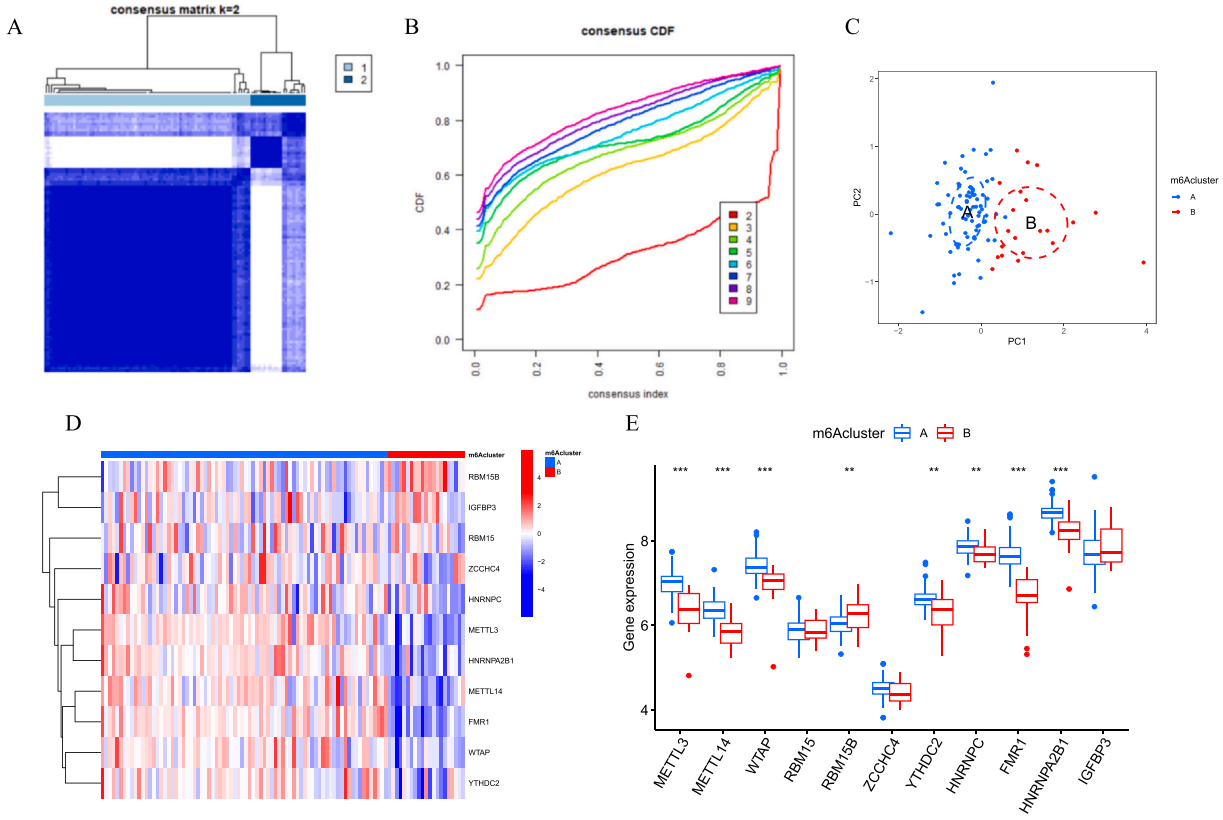

Fig. 5. Clustering analysis of 11 differentially expressed m6A regulatory genes. (A) Consensus matrices showing the clustering of DM-associated m6A regulatory genes when k = 2. (B) The cumulative distribution function shows different performances for k values ranging from 2 to 9, with k = 2 exhibiting the smallest descending order in the CDF curve. (C) Principal component analysis (PCA) of two m6A subtypes. (D, E) Heatmaps and box plots showing the status of 11 differentially expressed m6A genes between subtype A and subtype B. *p < 0.05, **p < 0.01, and ***p < 0.001.

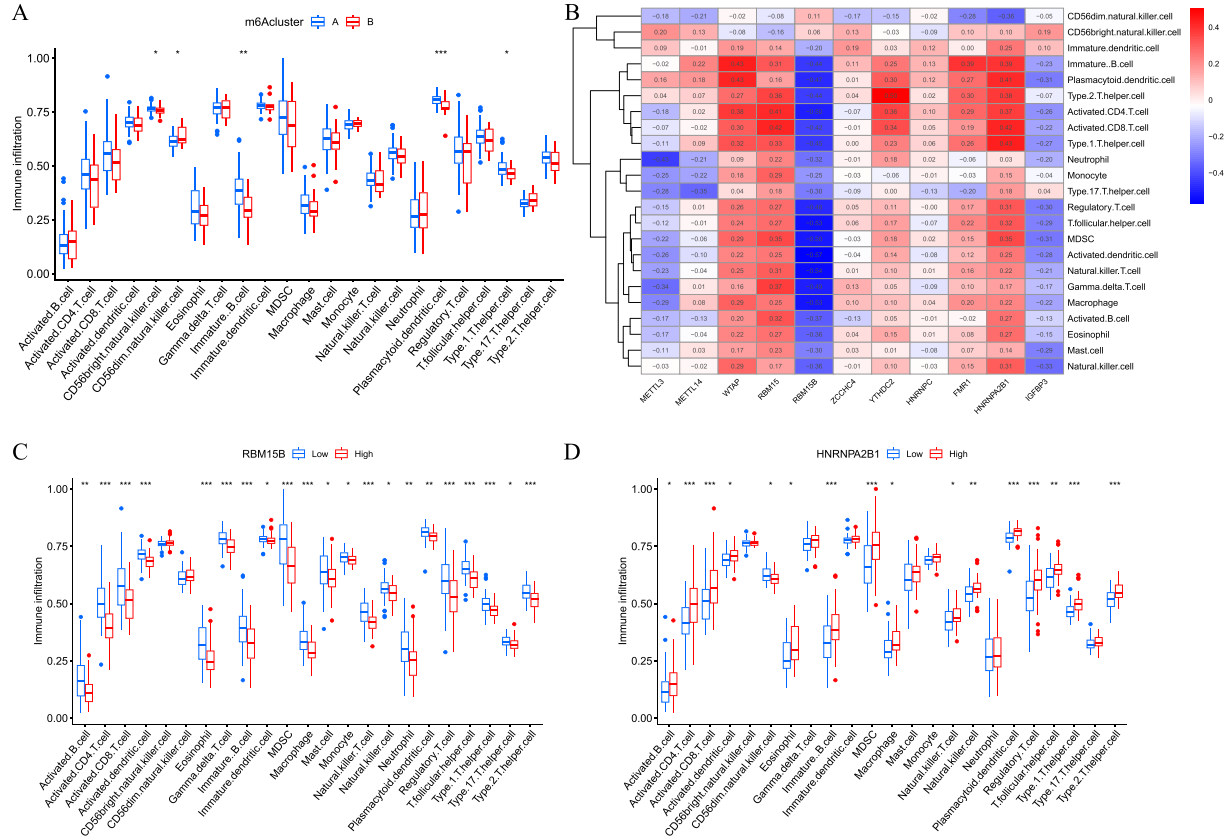

Fig. 6. Single Sample Gene Set Enrichment Analysis (ssGSEA) of two m6A modification subtypes. (A) Comparison of immune cell abundances between subtypes A and B. (B) Heatmap of m6A-regulated genes and immune cell infiltration. (C, D) Differences in immune cell infiltration between clusters with low and high expression of two m6A genes. *p < 0.05, **p < 0.01, and ***p < 0.001.

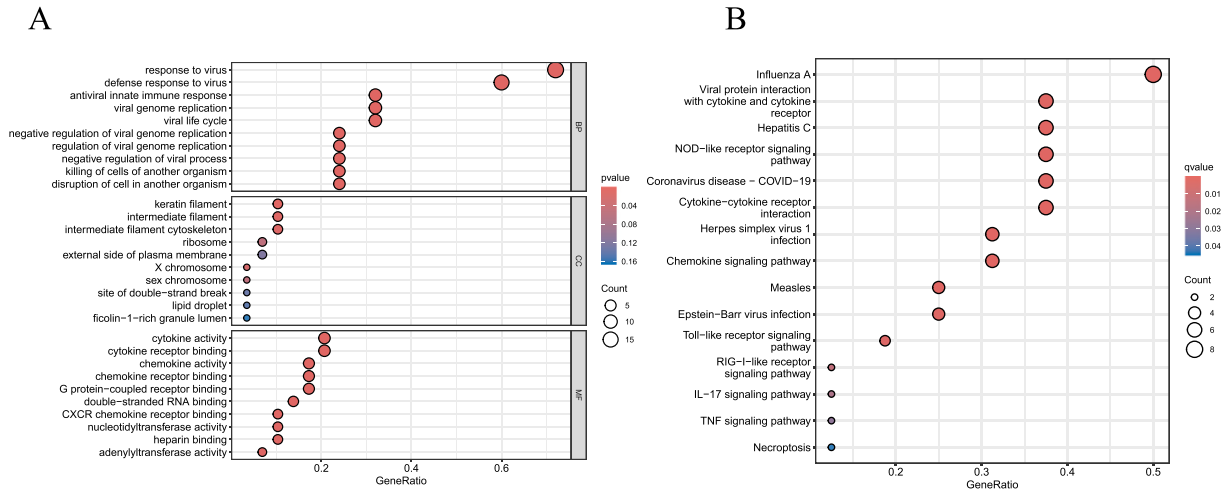

Fig. 7. Enrichment analysis of genes differentially expressed between m6A subtypes. (A) Gene Ontology (GO) analysis of these differentially expressed genes. (B) Kyoto Encyclopedia of Genes and Genomes (KEGG) pathway analysis of these genes.

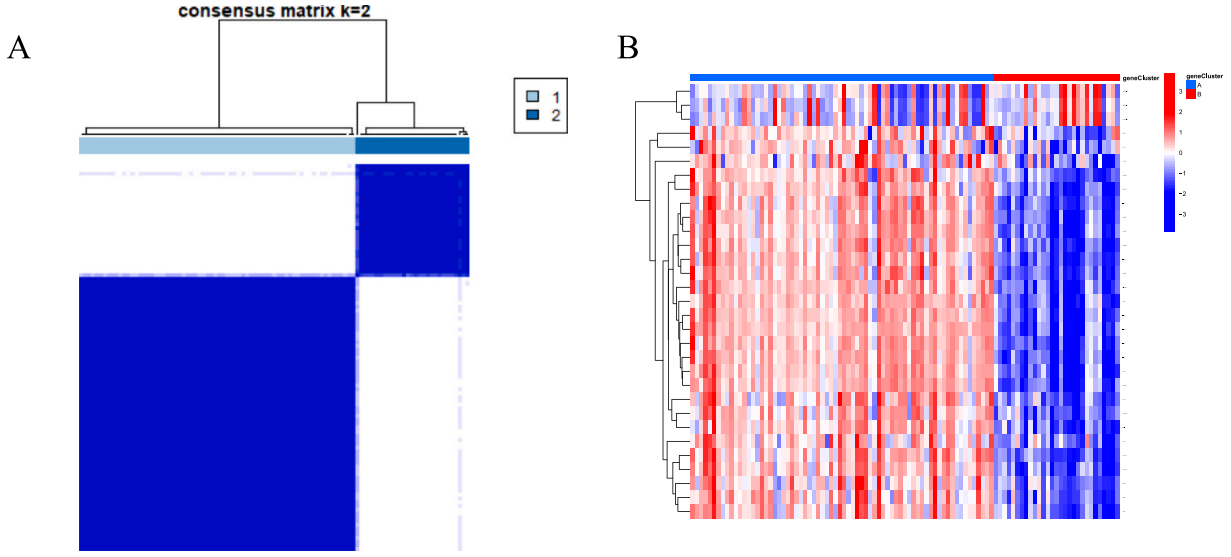

Fig. 8. Consensus clustering of genes differentially expressed between m6A subtypes. (A) Consensus matrices of these differentially expressed genes (k = 2). (B) Expression heatmap of genes differentially expressed between gene cluster A and gene cluster B.

In recent years, immune cell infiltration, autoantibodies, complement system disorders, and interferon signaling have been shown to collectively contribute to the pathogenesis of dermatomyositis [45]. Muscle biopsies in DM show that the microenvironment is enriched with myeloid and plasmacytoid antigen-presenting cells, alongside the overexpression of immune mediators such as Toll-like receptors. These factors and cells may lead to nuclear factor κB (NF-κB) aggregation, resulting in the overexpression of IFN-1 in dermatomyositis and further inflammatory damage [46]. Research by Radke et al. has also shown that IFN-1-related gene expression levels correlate with B-cell content in dermatomyositis tissue [47]. We categorized dermatomyositis samples into 2 subtypes based on 11 differentially expressed m6A genes. Significant differences in the level of infiltration among CD56 bright natural killer cells, CD56 dim natural killer cells, immature B cells, plasmacytoid dendritic cells, and type 1 T helper cells were also revealed between different m6A subtypes. In diseases such as SLE and pSS, an elevated ratio of CD56bright/CD56dim cells in peripheral blood indicates a more pronounced inflammatory response [48,49]. In neurological autoimmune disorders like MS, both subsets participate in regulating T/B lymphocyte activity [50]. However, direct evidence supporting the stratification of dermatomyositis (DM) subtypes based on CD56dim NK cells remains limited. We hypothesize that the observed differences in CD56dim NK cell abundance across DM subtypes may reflect variations in the tissue microenvironment, chemokine expression profiles, and associated signaling pathways. Previous studies have suggested that upregulation of chemokines such as CLA, CCR5, and CXCR6 may promote the migration of specific NK cell subsets to the skin, potentially contributing to distinct infiltration patterns across different DM subtypes [51]. Further large-scale, multicenter basic and translational studies focusing on diverse clinical phenotypes of DM are warranted to validate these speculations. This integration of m6A modification patterns with immune characteristics highlights a potential interplay between epigenetic regulation and the immune response, offering new insights for patient stratification. Further analysis of two genes, RBM15B and HNRNPA2B1, which were prominent in the immune cell correlation heatmap, revealed that most immune cell infiltration was significantly elevated in the group with low RBM15B expression, while HNRNPA2B1 expression showed consistency with immune cell

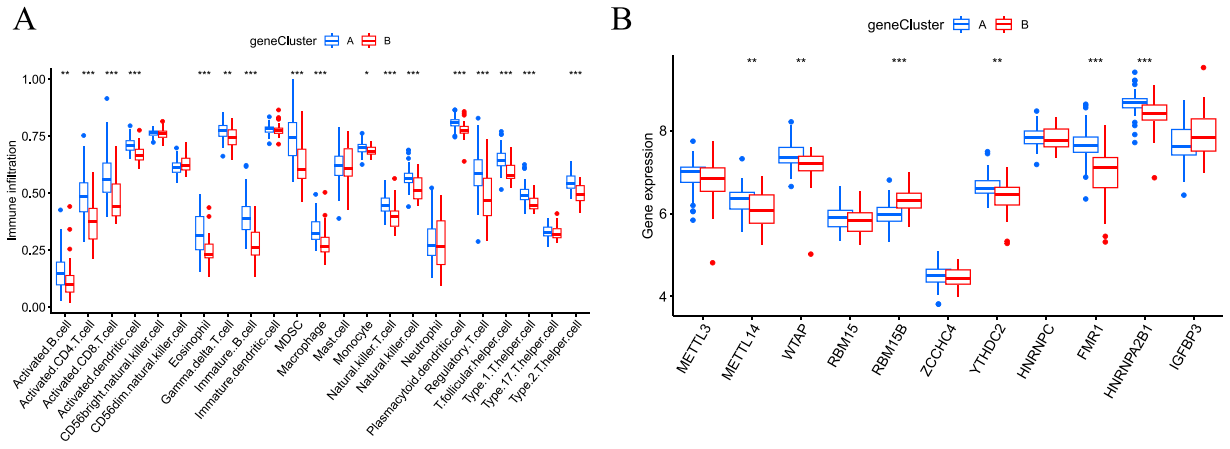

Fig. 9. Single Sample Gene Set Enrichment Analysis (ssGSEA) of two gene clusters. (A) Expression boxplot of DM-associated regulatory genes between two gene clusters. (B) Differences in the abundances of immune cells in the two gene clusters. *p < 0.05, **p < 0.01, and ***p < 0.001.

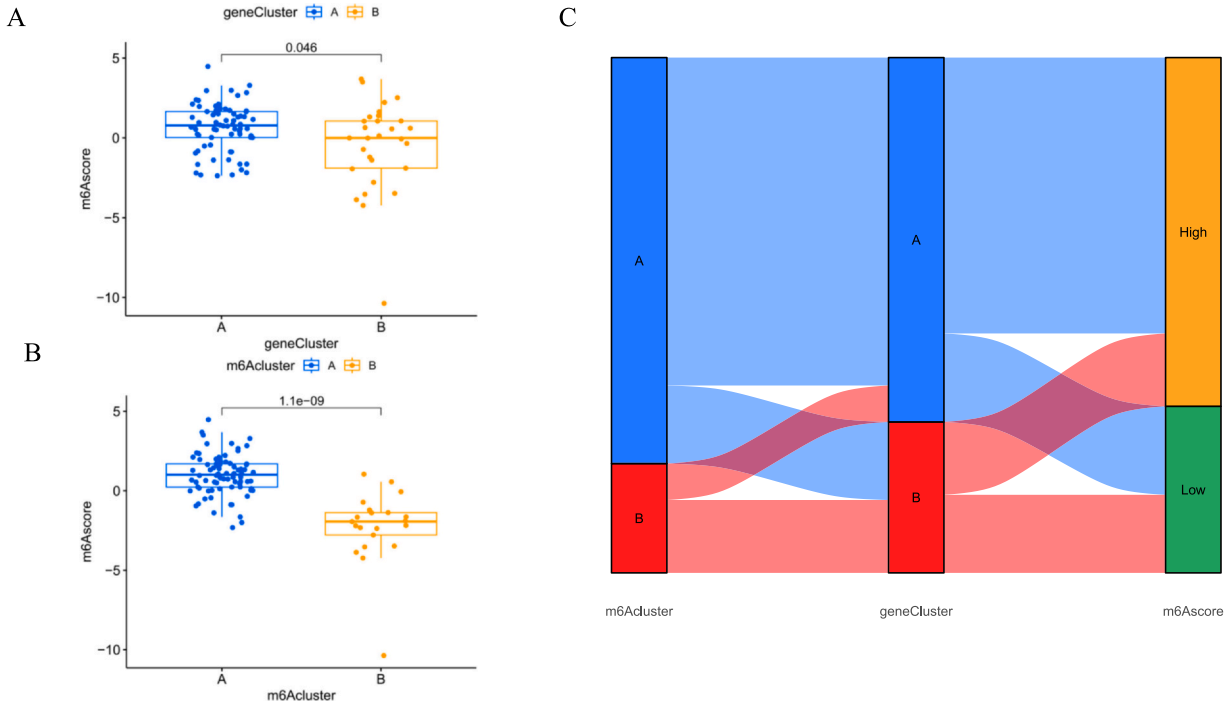

Fig. 10. m6A Scoring and Sankey Diagram. (A) Variation in m6A scores among A and B gene subtypes. (B) Variation in m6A scores among A and B m6A subtypes. (C) Sankey diagram demonstrating the consistent relationship among m6A subtypes, m6A gene subtypes, and m6A scores.

infiltration. This correlation pattern, which aligns with the observations in Fig. 2, further supports a potential association between m6A modification and the immune infiltration characteristics in dermatomyositis.

Similar to other autoimmune diseases, the development of dermatomyositis typically arises from the combined effects of exogenous triggering factors such as viral infections and susceptible genes [52]. Cases of dermatomyositis occurring after COVID-19 infection have been documented [53]. Additionally, Coxsackie virus, parvovirus, and HIV have all been identified as potential triggering factors [54,55]. Natasha holds the view that the autoantibodies in patients are the vestiges left by past infections [56]. Pathogens trigger an immune response in muscle tissue, and this response persists even after the microbes have been eradicated. In this study, enrichment analysis of genes differentially expressed between the two m6A subtypes was conducted. Gene ontology (GO) results showed enrichment primarily in processes such as defense responses to viruses, the cytoskeleton, cytokines, and receptor responses. The Kyoto Encyclopedia of Genes and Genomes (KEGG) analysis indicated that the pathways related to the influenza A virus were significantly enriched. These findings raise the possibility that m6A modifications may play a role in modulating the virus-associated immune response, which could be a contributing factor in the pathogenesis of dermatomyositis. These results are consistent with previous findings. Although direct evidence linking the influenza A virus to dermatomyositis remains scarce, our study provides novel insights into the pathogenesis of dermatomyositis.

Based on the differential genes between m6A subtypes, we performed secondary genotyping and successfully reproduced the binary classification. We speculate that m6A genes may regulate downstream differentially expressed genes. Significant differences in m6A scores between different m6A subtypes corresponded to their m6A expression variations. Significant m6A score variations were observed across gene subtypes, collectively suggesting the

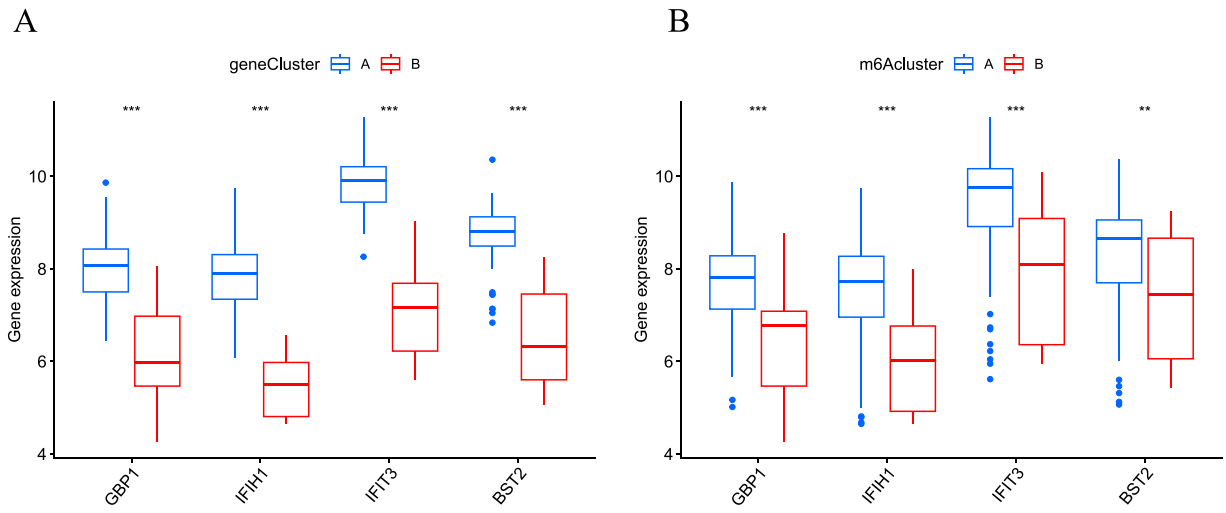

Fig. 11. Box plots of the expression of genes specific to different subtypes. (A) Expression levels of GBP1, IFIH1, IFIT3, and BST2 between gene subtypes. (B) Expression levels of GBP1, IFIH1, IFIT3, and BST2 between m6A subtypes. *p < 0.05, **p < 0.01, and ***p < 0.001.

possibility of a regulatory role for the m6A gene on downstream differentially expressed genes. However, these preliminary findings require experimental validation.

In conclusion, our study provides the first in-depth exploration of m6A regulation in dermatomyositis, offering novel insights into dermatomyositis pathogenesis and new perspectives for future dermatomyositis subtyping, risk assessment, and treatment. There are several limitations to our study. Firstly, due to the constrained sample size of the GEO database, batch effects were introduced when three GEO datasets were merged. We were unable to adjust for confounding factors, including age, gender, and infection. Second, as dermatomyositis encompasses clinical subtypes (e.g., anti-MDA5 dermatomyositis), the absence of suitable GEO cohorts precluded further analysis of clinical subtypes. Most importantly, additional experiments to verify the molecular mechanism of m6A in dermatomyositis are required. Future studies will address these limitations.

Conclusions

In summary, the various expression of m6A regulatory genes significantly influences the pathogenesis of dermatomyositis. We propose m6A-associated subtyping and gene subtyping, and construct a nomogram model to predict the risk of dermatomyositis. We provide the predictions for further mechanistic studies and therapeutic strategies.

Author contribution

Rui Tu and Youxian He designed the whole study, collected and analyzed the data, and revised the manuscript. Xiang Long and Yidan Hu analyzed the data, searched the literature, and drafted the manuscript. All authors contributed to this work and approved the final manuscript. Corresponding authors: Youxian He and Rui Tu.

Ethics approval and consent to participate

Research involving human data has been performed in accordance with the Declaration of Helsinki and approved by the Ethics Committee of the Fourth Affiliated Hospital of Southwest Medical University. It is noted that informed consent was obtained from the patients and individuals involved in the original studies.

Funding

This research did not receive any specific grant from funding agencies in the public, commercial, or not-for-profit sectors.

Declaration of Competing Interest

The authors declare that they have no known competing financial interests or personal relationships that could have appeared to influence the work reported in this paper.

Acknowledgements

We express our gratitude to all authors who have publicized data for the GEO dataset and to the participants included in the research.

Appendix A. Supporting information

Supplementary data associated with this article can be found in the online version at doi:10.1016/j.gmg.2026.100097.

References

[1] A.A. Amato, Intravenous immune globulin therapy in dermatomyositis[J], N. Engl. J. Med. 387 (14) (2022) 1320–1321, https://doi.org/10.1056/NEJMe2209117
[2] L. Cassard, N. Seraly, M. Riegert, et al., Dermatomyositis: practical guidance and unmet needs[J], Immunotargets Ther. 13 (2024) 151–172, https://doi.org/10.2147/itt.S381472
[3] S. Davuluri, L. Chung, C. Lood, Calcinosis in dermatomyositis[J], Curr. Opin. Rheuma 36 (6) (2024) 453–458, https://doi.org/10.1097/bor.0000000000001036
[4] S. Chen, H. Li, H. Zhan, et al., Identification of hub biomarkers and immune cell infiltration in polymyositis and dermatomyositis[J], Aging (Albany NY) 14 (10) (2022) 4530–4555, https://doi.org/10.18632/aging.204098
[5] E.F. Martins, C.H. Cappello, S.K. Shinjo, et al., Idiopathic inflammatory myopathies: recent evidence linking pathogenesis and clinical features[J], Int J. Mol. Sci. 26 (7) (2025), https://doi.org/10.3390/ijms26073302
[6] C. Liu, Y. Ge, Immune-related genes associated with interstitial lung disease in dermatomyositis[J], Int J. Gen. Med 17 (2024) 5261–5271, https://doi.org/10.2147/ijgm.S490294
[7] N. Seto, J.J. Torres-Ruiz, C. Carmona-Rivera, et al., Neutrophil dysregulation is pathogenic in idiopathic inflammatory myopathies[J], JCI Insight 5 (3) (2020), https://doi.org/10.1172/jci.insight.134189
[8] L. Bolko, C. Gitiaux, Y. Allenbach, [Dermatomyositis: new antibody, new classification][J], Hors série n° 2, Med. Sci. 35 (2019) 18–23, https://doi.org/10.1051/medsci/2019178
[9] J.N. Kuehner, J. Chen, E.C. Bruggeman, et al., 5-hydroxymethylcytosine is dynamically regulated during forebrain organoid development and aberrantly altered in Alzheimer's disease[J], Cell Rep. 35 (4) (2021) 109042, https://doi.org/10.1016/j.celrep.2021.109042

[10] Z.H. Feng, Y.P. Liang, J.J. Cen, et al., m6A-immune-related lncRNA prognostic signature for predicting immune landscape and prognosis of bladder cancer[J], J. Transl. Med. 20 (1) (2022) 492, https://doi.org/10.1186/s12967-022-03711-1

[11] Y. Zhang, L.X. Gao, W. Wang, et al., M(6) A demethylase fat mass and obesity-associated protein regulates cisplatin resistance of gastric cancer by modulating autophagy activation through ULK1[J], Cancer Sci. 113 (9) (2022) 3085–3096, https://doi.org/10.1111/cas.15469

[12] L. Cui, R. Ma, J. Cai, et al., RNA modifications: importance in immune cell biology and related diseases[J], Signal Transduct. Target Ther. 7 (1) (2022) 334, https://doi.org/10.1038/s41392-022-01175-9

[13] Y. Huang, Q. Xue, J. Chang, et al., M6A methylation modification in autoimmune diseases, a promising treatment strategy based on epigenetics[J], Arthritis Res. Ther. 25 (1) (2023) 189, https://doi.org/10.1186/s13075-023-03149-w

[14] X. Jiang, B. Liu, Z. Nie, et al., The role of m6A modification in the biological functions and diseases[J], Signal Transduct. Target Ther. 6 (1) (2021) 74, https://doi.org/10.1038/s41392-020-00450-x

[15] Z. Shulman, N. Stern-Ginossar, The RNA modification N(6)-methyladenosine as a novel regulator of the immune system[J], Nat. Immunol. 21 (5) (2020) 501–512, https://doi.org/10.1038/s41590-020-0650-4

[16] C. Zhang, Y. Chen, B. Sun, et al., m(6)A modulates haematopoietic stem and progenitor cell specification[J], Nature 549 (7671) (2017) 273–276, https://doi.org/10.1038/nature23883

[17] J. Lv, Y. Zhang, S. Gao, et al., Endothelial-specific m(6)A modulates mouse hematopoietic stem and progenitor cell development via Notch signaling[J], Cell Res 28 (2) (2018) 249–252, https://doi.org/10.1038/cr.2017.143

[18] Q. Geng, X. Cao, D. Fan, et al., Diagnostic gene signatures and aberrant pathway activation based on m6A methylation regulators in rheumatoid arthritis[J], Front Immunol. 13 (2022) 1041284 ,https://doi.org/10.3389/fimmu.2022.1041284

[19] W. Shi, Y. Zheng, S. Luo, et al., METTL3 Promotes Activation and Inflammation of FLSs Through the NF-κB Signaling Pathway in Rheumatoid Arthritis[J], Front Med. (Lausanne) 8 (2021) 607585, https://doi.org/10.3389/fmed.2021.607585

[20] J. Wu, L.J. Deng, Y.R. Xia, et al., Involvement of N6-methyladenosine modifications of long noncoding RNAs in systemic lupus erythematosus[J], Mol. Immunol. 143 (2022) 77–84, https://doi.org/10.1016/j.molimm.2022.01.006

[21] Y. Chen, M. Shen, C. Ji, et al., Genome-Wide Identification of N6-Methyladenosine Associated SNPs as Potential Functional Variants for Type 1 Diabetes[J], Front Endocrinol. (Lausanne) 13 (2022) 913345 , https://doi.org/10.3389/fendo.2022.913345

[22] F. Ye, T. Wang, X. Wu, et al., N6-Methyladenosine RNA modification in cerebrospinal fluid as a novel potential diagnostic biomarker for progressive multiple sclerosis[J], J. Transl. Med. 19 (1) (2021) 316, https://doi.org/10.1186/s12967-021-02981-5

[23] S. Li, H. Liu, Z. Ruan, et al., Landscape analysis of m6A modification regulators related biological functions and immune characteristics in myasthenia gravis[J], J. Transl. Med. 21 (1) (2023) 166, https://doi.org/10.1186/s12967-023-03947-5

[24] D. Li, Y. Li, K. Zhu, et al., Analysis of m6A-regulated genes and subtype classification in lupus nephritis[J], BMC Nephrol. 25 (1) (2024) 119, https://doi.org/10.1186/s12882-024-03549-3

[25] X. Zhong, J. Shang, R. Zhang, et al., Explore the shared molecular mechanism between dermatomyositis and nasopharyngeal cancer by bioinformatic analysis[J], PLoS One 19 (5) (2024) e0296034 ,https://doi.org/10.1371/journal.pone.0296034

[26] Y. Jiang, Y. Liu, Y. Zhao, et al., Mitochondrial morphology and MAVS-IFN1 signaling pathway in muscles of anti-MDA5 dermatomyositis[J], Ann. Clin. Transl. Neurol. 8 (3) (2021) 677–686, https://doi.org/10.1002/acn3.51311

[27] Q.L. Peng, Y.M. Zhang, L. Liang, et al., A high level of serum neopterin is associated with rapidly progressive interstitial lung disease and reduced survival in dermatomyositis[J], Clin. Exp. Immunol. 199 (3) (2020) 314–325, https://doi.org/10.1111/cei.13404

[28] V.L. Kronzer, B.A. Kimbrough, C.S. Crowson, et al., Incidence, prevalence, and mortality of dermatomyositis: a population-based cohort study[J], Arthritis Care Res. (Hoboken) 75 (2) (2023) 348–355, https://doi.org/10.1002/acr.24786

[29] J. Wienke, L.M. Pachman, G.A. Morgan, et al., Endothelial and Inflammation Biomarker Profiles at Diagnosis Reflecting Clinical Heterogeneity and Serving as a Prognostic Tool for Treatment Response in Two Independent Cohorts of Patients With Juvenile Dermatomyositis[J], Arthritis Rheuma 72 (7) (2020) 1214–1226, https://doi.org/10.1002/art.41236

[30] K.Y. Sun, Y. Fan, Y.X. Wang, et al., Prevalence of interstitial lung disease in polymyositis and dermatomyositis: A meta-analysis from 2000 to 2020[J], Semin Arthritis Rheum. 51 (1) (2021) 175–191, https://doi.org/10.1016/j.semarthrit.2020.11.009

[31] D. Didona, F. Solimani, R.D. Caposiena Caro, et al., Dermatomyositis: a comprehensive review of clinical manifestations, serological features, and therapeutic approaches[J], Ital. J. Dermatol. Venerol. 158 (2) (2023) 84–98, https://doi.org/10.23736/s2784-8671.23.07458-3

[32] S. Santourlidis, Phyloepigenetics[J], Biology 11 (5) (2022), https://doi.org/10.3390/biology11050754

[33] R. Bechara, S.L. Gaffen, '(m(6))A' stands for 'autoimmunity': reading, writing, and erasing RNA modifications during inflammation[J], Trends Immunol. 42 (12) (2021) 1073–1076, https://doi.org/10.1016/j.it.2021.10.002

[34] C.M. Huang, Y.C. Chen, I.L. Lai, et al., Exploring RNA modifications, editing, and splicing changes in hyperuricemia and gout[J], Front. Med. (Lausanne) 9 (2022) 889464, https://doi.org/10.3389/fmed.2022.889464

[35] F. Truffinet, A. Arco-Hierves, H. Shalabi, et al., m(6)A RNA methylation controls salivary gland epithelial cell function and has a protective role in Sjögren's disease[J], Ann. Rheum. Dis. (2024), https://doi.org/10.1136/ard-2024-226224

[36] Y. He, Y. Hu, M. Yuan, et al., Prognostic and therapeutic implication of m6A methylation in Crohn disease[J], Med. (Baltim.) 101 (51) (2022) e32399, https://doi.org/10.1097/md.0000000000032399

[37] Q. Luo, J. Rao, L. Zhang, et al., The study of METTL14, ALKBH5, and YTHDF2 in peripheral blood mononuclear cells from systemic lupus erythematosus[J], Mol. Genet Genom. Med 8 (9) (2020) e1298 ,https://doi.org/10.1002/mgg3.1298

[38] Z. Zhu, L. Wan, N6-methyladenosine methyltransferase METTL14 is associated with macrophage polarization in rheumatoid arthritis[J], Exp. Ther. Med. 28 (4) (2024) 375, https://doi.org/10.3892/etm.2024.12664

[39] M. Fakhar, M. Gul, W. Li, Structural and Functional Studies on Key Epigenetic Regulators in Asthma[J], Biomolecules 15 (9) (2025), https://doi.org/10.3390/biom15091255

[40] D.P. Patil, C.K. Chen, B.F. Pickering, et al., m(6)A RNA methylation promotes XIST-mediated transcriptional repression[J], Nature 537 (7620) (2016) 369–373, https://doi.org/10.1038/nature19342

[41] Y. Xu, Y. Zhang, Y. Luo, et al., Novel insights into the METTL3-METTL14 complex in musculoskeletal diseases[J], Cell Death Discov. 9 (1) (2023) 170, https://doi.org/10.1038/s41420-023-01435-9

[42] S. Suzuki, S. Morimoto, M. Fujishiro, et al., Inhibition of the insulin-like growth factor system is a potential therapy for rheumatoid arthritis[J], Autoimmunity 48 (4) (2015) 251–258, https://doi.org/10.3109/08916934.2014.976631

[43] A. Ayoufu, L. Yi, M. Tuersuntuoheti, et al., HNRNPA2B1 is a potential biomarker of breast cancer related to prognosis and immune infiltration[J], Aging (Albany NY) 15 (17) (2023) 8712–8728, https://doi.org/10.18632/aging.204992

[44] Z. Gu, Y. Yang, Q. Ma, et al., HNRNPC, a predictor of prognosis and immunotherapy response based on bioinformatics analysis, is related to proliferation and invasion of NSCLC cells[J], Respir. Res 23 (1) (2022) 362, https://doi.org/10.1186/s12931-022-02227-y

[45] R.G. Kamperman, A.J. van der Kooi, M. de Visser, et al., Pathophysiological Mechanisms and Treatment of Dermatomyositis and Immune Mediated Necrotizing Myopathies: A Focused Review[J], Int. J. Mol. Sci. 23 (8) (2022), https://doi.org/10.3390/ijms23084301

[46] S.A. Greenberg, Dermatomyositis and type 1 interferons[J], Curr. Rheuma Rep. 12 (3) (2010) 198–203, https://doi.org/10.1007/s11926-010-0101-6

[47] J. Radke, R. Koll, C. Preuße, et al., Architectural B-cell organization in skeletal muscle identifies subtypes of dermatomyositis[J], Neurol. Neuroimmunol. Neuroinflamm. 5 (3) (2018) e451, https://doi.org/10.1212/nxi.0000000000000451

[48] H. Li, L. Geng, Z. Cao, et al., CD56brightCD16- to CD57+CD56dimCD16+ NK cell ratio discriminates disease activity and renal involvement in patients with systemic lupus erythematosus[J], Clin. Exp. Rheuma 41 (9) (2023) 1768–1776, https://doi.org/10.55563/clinexprheumatol/o6bjl8

[49] B. Ming, T. Wu, S. Cai, et al., The Increased Ratio of Blood CD56(bright) NK to CD56(dim) NK Is a Distinguishing Feature of Primary Sjögren's Syndrome[J], J. Immunol. Res 2020 (2020) 7523914, https://doi.org/10.1155/2020/7523914

[50] S. Rodríguez-Lorenzo, L. van Olst, C. Rodriguez-Mogeda, et al., Single-cell profiling reveals periventricular CD56(bright) NK cell accumulation in multiple sclerosis[J], Elife 11 (2022), https://doi.org/10.7554/eLife.73849

[51] A. Zaid, J.L. Hor, S.N. Christo, et al., Chemokine Receptor-Dependent Control of Skin Tissue-Resident Memory T Cell Formation[J], J. Immunol. 199 (7) (2017) 2451–2459, https://doi.org/10.4049/jimmunol.1700571

[52] M. Schorer, K. Lambert, N. Rakebrandt, et al., Rapid expansion of Treg cells protects from collateral colitis following a viral trigger[J], Nat. Commun. 11 (1) (2020) 1522, https://doi.org/10.1038/s41467-020-15309-6

[53] B.V.K. Ho, E.W. Seger, K. Kollmann, et al., Dermatomyositis in a COVID-19 positive patient[J], JAAD Case Rep. 13 (2021) 97–99, https://doi.org/10.1016/j.jdcr.2021.04.036

[54] J.F. Boehler, A. Horn, J.S. Novak, et al., Mitochondrial dysfunction and role of harakiri in the pathogenesis of myositis[J], J. Pathol. 249 (2) (2019) 215–226, https://doi.org/10.1002/path.5309

[55] T.E. Lloyd, I. Pinal-Fernandez, E.H. Michelle, et al., Overlapping features of polymyositis and inclusion body myositis in HIV-infected patients[J], Neurology 88 (15) (2017) 1454–1460, https://doi.org/10.1212/wnl.0000000000003821

[56] I.R. Mackay, N.V. Leskovsek, N.R. Rose, Cell damage and autoimmunity: a critical appraisal[J], J. Autoimmun. 30 (1-2) (2008) 5–11, https://doi.org/10.1016/j.jaut.2007.11.009